Finite Element Analysis of CFFT and CFDTS Columns as a Replacement for CFST Columns in Composite Construction by Using ABAQUS

Sah, R.
Nepal Polytechnic Institute, Bharatpur, Chitwan, Nepal
Corresponding Email: ranjeetsah138@gmail.com

Abstract

In the field of composite construction of steel and concrete, concrete filled steel tube CFST columns have been proven to be greater performance structural members. The properties of steel and concrete are used efficiently. But CSFT columns are prone to corrosion in outdoor structures as the outer encasing tube is made up of steel. The outdoor use of CFST column due to its high risk of corrosion requires frequent maintenance and may prove costly. Hence, the possible replacement of steel tubes with fiber-reinforced polymer (FRP) Tubes has to be investigated. FRPs are the most suitable material for encasing concrete columns due to its orthotropic behaviour. In solution to this, the paper is aimed at numerical study of CFST, CFFT and CFDTS short columns to study the axial compression behavior of these short columns analytically and examine the best suitable alternatives of CFST column. The concrete in-fill double tube section CFDTS with better axial compression, stiffness and ductility are also investigated as a suitable replacement of CFST columns. For these three different specimens of CFST columns of steel tube thickness 3mm, 4.5mm and 6mm, CFFT columns of GFRP tube thickness 3mm, 4.5mm and 6mm and CFDTS column with GFRP outer tube of thickness 3mm, 4.5mm and 6mm as well as inner steel tube of thickness 1.5mm, 2mm and 2.5mm are analyzed and compared. Consequently, CFDTS columns, with 1872 kN are proven to be superior to CFST columns with axial capacity 1653 kN and CFFT with axial capacity 689 kN columns. The confinement effect in CFDTS is more than CFST and CFFT column.

Keywords: CFST columns, CFFT columns, CFDTS columns, GFRP tube, Finite Element Analysis

Introduction

Civil construction industry has outlined a number of materials which exhibits excellent structural behaviors when used in structure. Amongst many such materials, steel and concrete makes the best composites construction material. In the field of steel and concrete composite construction, Concrete filled Steel Tube CFST columns have been proven to be greater performance structural members (Qasim S. Khan, M. Neaz Sheikh, 2020). The properties of steel and concrete are used efficiently. The ductile behavior of steel tube and impressive compression characteristic of concrete makes a rigid, semi ductile steel concrete composite column. In circular CFST columns, due to confinement effect concrete is stressed in tri-axial state and this allows the concrete to exhibit greater compression performance compared to unconfined concrete. The combination of ductile property of steel, confined tri-axial higher compression behavior of concrete give rise to a structural member with better strength, stiffness and ductility (Mimiran & Shahaway, 1997).

But when used in harsh marine environment, the inevitable pitting corrosion poses a crucial threat to the outer surface of CFST and results in stress concentration, early local buckling as well as confinement reduction towards concrete. The effect of corrosion on the performance and strength of CFST column due to localized pitting corrosion, uniform corrosion and un-corroded is studied by *Gen Li et.al.* (Li et al., 2022) and found that a more severe degradation in strength is caused by localized pitting corrosion than uniform corrosion. They concluded that the corrosion of steel tube has significant role in reduction in design capacity of CFST column. This study aims to give a better solution to the above mentioned problem associated with CFST column. Here, the Concrete Filled Glass Fiber Reinforced Polymer Tubes CFFT column is investigated for its mechanical behavior as a replacement of classical steel tube. The main objective of this study is to illustrate Concrete Filled Double Tube Section CFDTS columns a best alternative of CFST columns. In larger scale if implemented could be economical.

Methodology

This work was aimed to examine the axial compression capacity of CFST, CFFT and CFDTS short columns and to compare their axial behaviour and numerically manifest that CFFT and CFDTS columns are the best alternative replacement of CFST column. For this, finite element analysis has been carried out on FE models of CFST, CFFT and CFDTS columns. The finite element analysis

software used is ABAQUS/CAE. The validations of the numerical results were done for some specimens by casting and testing in structural Lab.

The objectives were accomplished in two approaches. They are:

- Validating the FEM models with experimental results
- Numerical Study of CFST, CFFT and Double section CFDTS

1.1 Validating the fem models with experimental results:

The validation of following specimens are carried out.

- Normal Concrete Cylinder of grade M25
- CFFT short column filled with concrete of grade M25
- CFST short column filled with concrete of grade M25

1.1.1 Material properties

The material properties used in modelling the specimens in ABAQUS/CAE are mentioned in the table below. The mechanical properties of the concrete are taken directly from Structural Engineering International Nr. 1/2017 (Hafezolghorani et al., 2017) are necessary input data for analysing the axial behaviour of CFST, CFFT and CFDTS short columns in ABAQUS/CAE.

Table 1. Load Vs. Displacement values

Displacement (mm)	Load (KN)
0	0
0.008	30
0.015	60
0.025	90
0.032	120
0.04	150
0.05	180
0.055	210
0.06	240
0.07	270
0.075	300
0.09	330
0.11	353.36

Table 2. Compressive Behaviour of M25 grade concrete

Stress (N/mm2)	Strain (mm/mm)
0.001	0.000000
1.698	0.000053
3.395	0.000100
5.093	0.000167
6.791	0.000213
8.488	0.000267
10.186	0.000333
11.884	0.000367
13.581	0.000400
15.279	0.000467
16.977	0.000500
18.674	0.000600
19.996	0.000733

Table 3. Tensile behaviour of Concrete

Yield Stress (N/mm2)	Cracking strain (mm/mm)
3.5	0
0.035	0.00014

Table 4. Plastic behaviour of Concrete

Material's Parameter	M25	Plastic Parameters (Hafezolghorani et al., 2017)	
Concrete Elasticity		Dilatation Angle	31
E (GPa)	25	Eccentricity	0.1
μ	0.2	fb0/fc0	1.16
		K	0.67
		Viscosity Parameter	0

Table 5. GFRP lamina properties: (Anitha Priyadharshani et al., 2017)

Young's Modulus in fiber in direction 11, E_{11} (MPa)	Young's Modulus in fiber in direction 2-2, E_{22} (MPa)	Poisson's ratio between fiber in direction 1-2, μ_{12}	Shear Modulus of fiber in direction 1-2, G_{12} (MPa)	Shear Modulus of fiber in direction 2-3, G_{23} (MPa)	Shear Modulus of fiber in direction 1-3, G_{13} (MPa)
11724	15087	0.16	4882	2333	2333

Table 6. Mechanical Behaviour of steel

Yield Stress (N/mm2)	Plastic Strain (mm/mm)
281.07	0
282.65	0.000286
284.22	0.000557
285.79	0.000829
301.59	0.00354
317.48	0.00623
333.45	0.00892
349.50	0.0116
365.64	0.0143

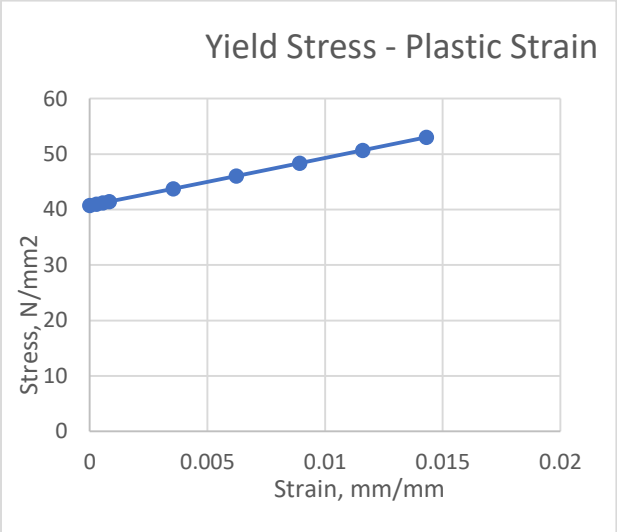

Fig (1): Stress-Plastic strain of steel

1.1.2 Finite element model and analysis

Finite element software ABAQUS/CAE was used to develop a FE model for CFST, CFFT and CFDTS columns(ABAQUS, 2014). An 8-noded triangular in-plane continuum shell wedge (SC8R) is used for GFRP tube, Shell Concrete, steel tube and the concrete core. For conducting nonlinear FE analysis, static general analysis based on Newton Raphson method is used (Kopuri & Priyadharshani, 2022). Interaction between the steel tube and concrete core is modeled in such a way that inner part of the steel tube is master surface and outer part of concrete core is slave surface. The coefficient of friction between the inner surface of the steel tube and outer surface of the concrete core is 0.6 for all columns specimens of CFST and CFFT(Hafezolghorani et al., 2017). However, in CFDTS a larger co-efficient of friction 0.8 is utilized to encounter de-bonding while analyzing in ABAQUS/CAE. The bottom portion of the specimens is modelled as a fixed end. Both the translation and rotational movement is restricted. The other end is modelled as a roller where displacement in Z direction is allowed. Therefore, the boundary conditions are: a) at fixed end $U_1=0$, $U_2=0$ & $U_3=0$ b) At the other end $U_1=0$, $U_2=0$, $U_3 \neq 0$.

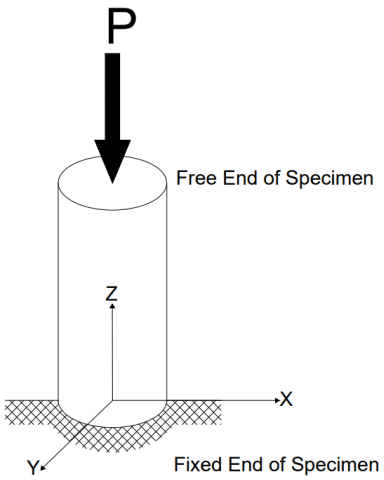

Fig (2): Boundary conditions of the specimen for FEM model

1.1.3 Validation of normal concrete cylinder

The concrete cylinder of the following dimensions was validated.

- Grade of In-filled Concrete = M25
- Diameter of specimen = 150 mm
- Gauge Length = 150mm
- Aspect ratio (L/D) = 2
- Height of Specimen (L) = 300 mm

Finite element Output

(1) Loading and Support conditions:

(2) Mesh

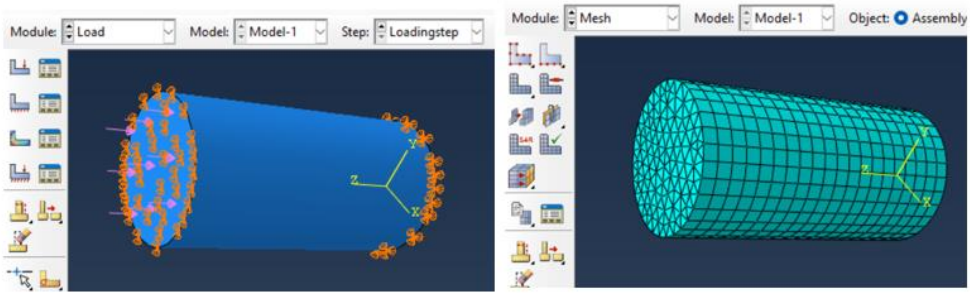

(3) Results from ABAQUS:

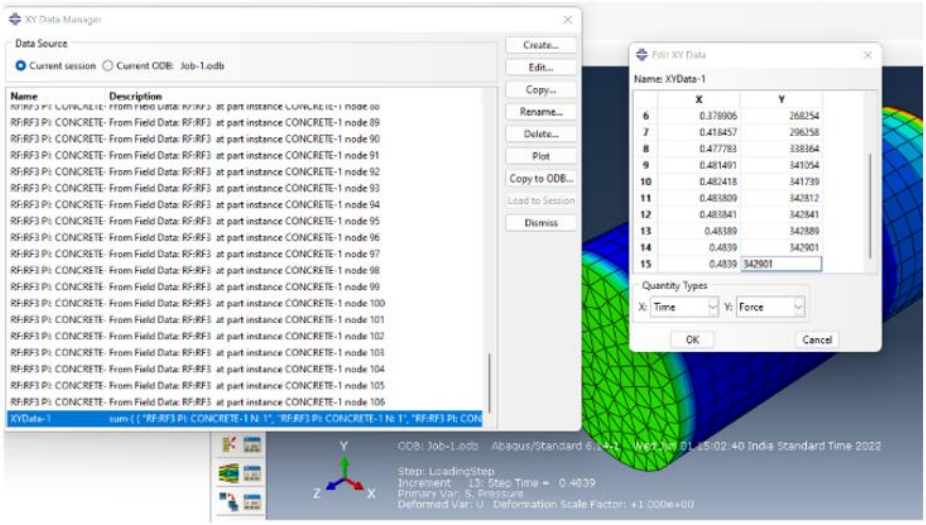

Fig (3): Abaqus model and output from Abaqus

Experimental Output:

a) b)

Fig (4): Lab test set up of Concrete cylinder a) before failure b) after failure

Comparison:

The results obtained from Finite Element Analysis Model and lab test are compared and checked for the possible differences. The calculated error should be < 10%.

The load vs. deformation variation

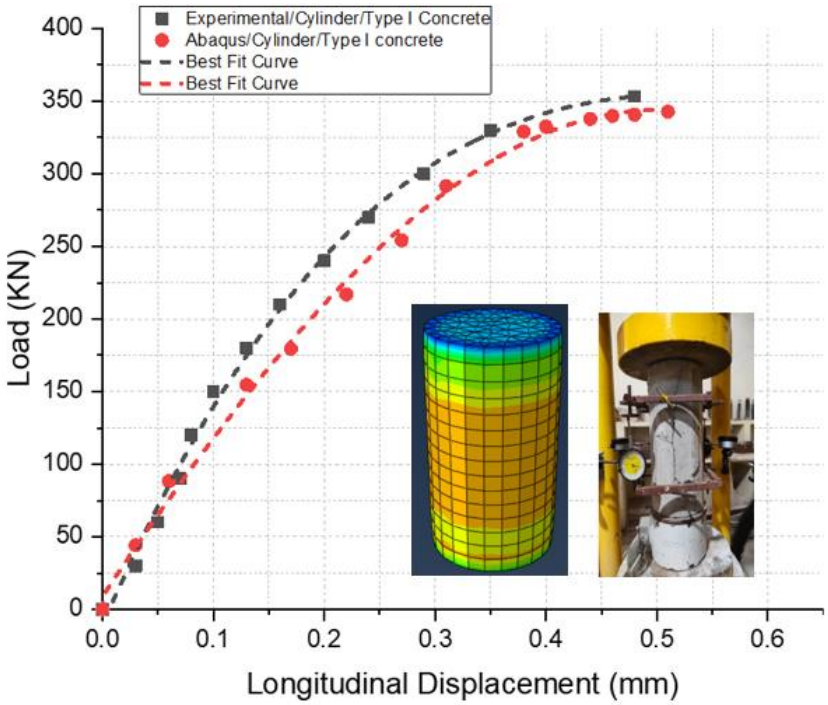

Fig (5): Load versus Longitudinal Deformation

- ABAQUS/CAE: The Capacity of concrete cylinder = **342.68 kN**
- Experimental: The Capacity of concrete cylinder = **353.36 kN**

The error in capacity of concrete cylinder is 3.02% which is less than the 10%. The results from Finite Element Analysis tool i.e. ABAQUS/CAE and experimental i.e. lab test are checked for their convergence and was found within the acceptable margins of error and hence validated.

1.1.4 Validation of cfft column

The concrete cylinder of the following dimensions was validated.

- Grade of In-filled Concrete = M_{25}
- External diameter of specimen = 152.4 mm

- Internal diameter of specimen = 143.4 mm
- Thickness of GFRP tube (t) = 4.5mm (6 Layers)
- Aspect ratio (L/D) = 3
- Height of Specimen (L) = 457.2 mm

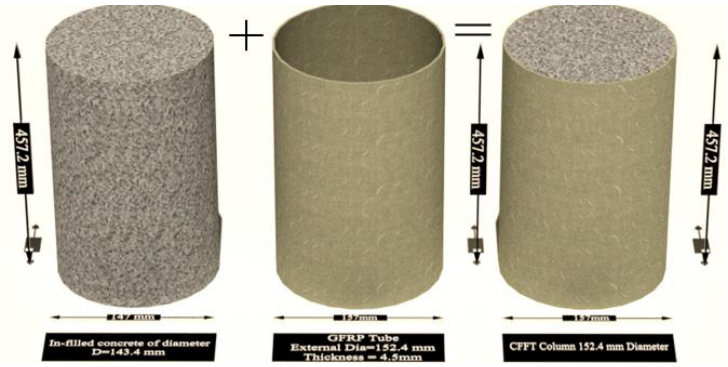

Fig (6): CFFT column for pictorial reference

GFRP tube is a brittle material and fails suddenly with a blasting sound. Thus, CFFT column check is based on strain theory.

The load vs. deformation variation

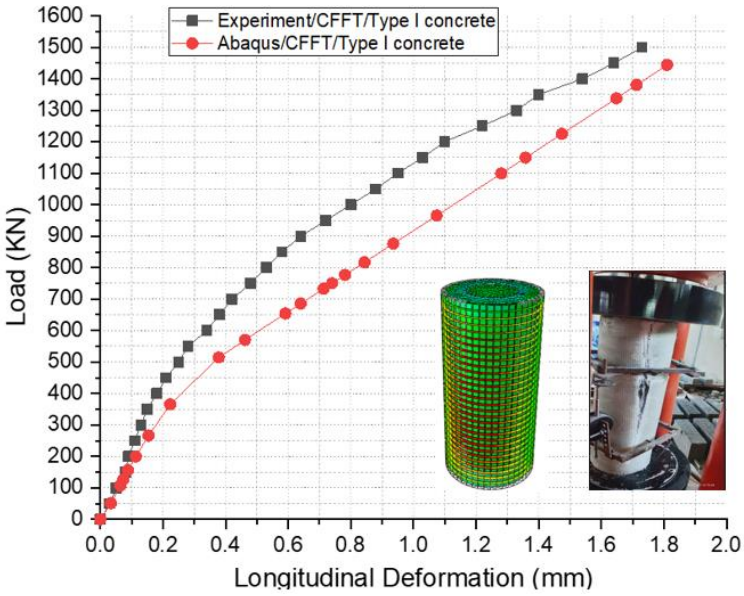

Fig (7): Comparison of Load-Deformation curve for CFFT in-filled with Concrete: Experimental Versus. ABAQUS/CAE

- ABAQUS/CAE: The Capacity of CFFT Column 4.5mm thick GFRP tube filled with concrete = **1444.04 kN**
- Lab Test: The Capacity of CFFT Column 4.5mm GFRP tube filled with concrete = **1500 kN**

The error in capacity of concrete cylinder is 3.7% which is less than the 10%. The results from Finite Element Analysis tool i.e. ABAQUS/CAE and experimental i.e. lab test are checked for their convergence and was found within the acceptable margins of error and hence validated.

1.1.5 Validation of cfst column

The concrete cylinder of the following dimensions was validated.

- Grade of In-filled Concrete = M25
- External diameter of specimen =152.4 mm
- Diameter of in-filled concrete = 149.4mm
- Thickness of Steel Tube =1.5mm
- Gauge Length =152.4mm
- Aspect ratio (L/D) =2
- Height of Specimen (L) =304.8 mm

Steel tube is a ductile material and fails by yielding. Thus CFST column check is based on stress theory.

The load vs. deformation variation

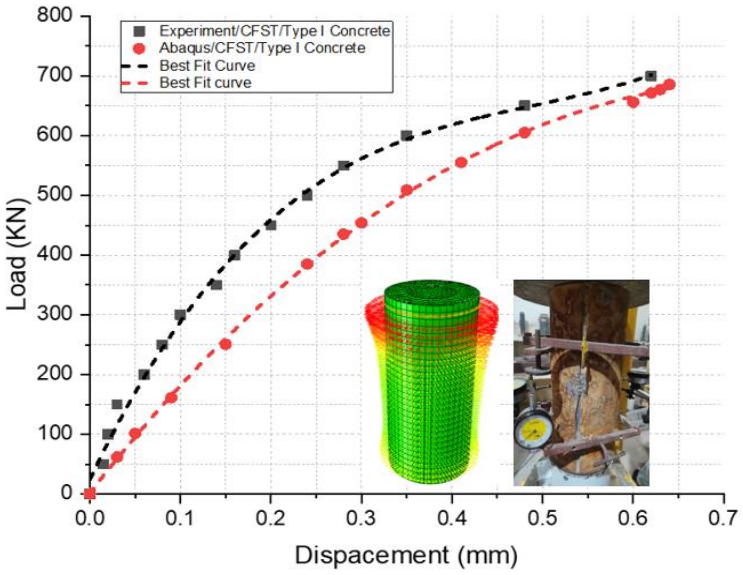

Fig (8): Comparison of Load-Deformation curve for CFST in-filled with Concrete from testing actual specimen from lab test and Abacus model.

- ABAQUS/CAE: Capacity of CFST Column 1.5mm thick Steel tube filled with concrete = **683.027 kN**
- Experimental: Capacity of CFST Column 1.5mm thick Steel tube filled with =**723 kN**

The error in capacity of concrete cylinder is 5.52% which is less than the 10%. The results from Finite Element Analysis tool i.e. ABAQUS/CAE and experimental i.e. lab test are checked for their convergence and was found within the acceptable margins of error and hence validated.

1.2 Analytical study of cfst, cfft and cfdts column using abaqus/cae

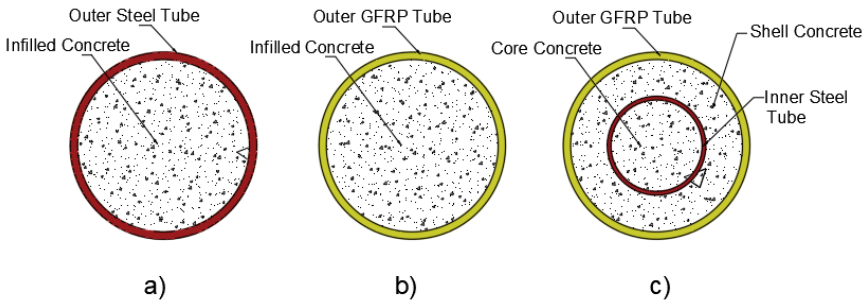

Fig (9) Concrete filled Steel tube column CFST b) Concrete filled GFRP tube column CFFT c) Concrete filled Double section (GFRP outer & steel inner tube) CFDTS column

The specification of the column specimen used for Finite Element Analysis.

Table 7. Concrete filled steel tube CFST column

Type of Specimen	Dia. of steel Tube (D_s)	Thickness of Steel tube, t_s (mm)	Aspect ratio (D_s/t_s)	Grade of In-filled Concrete
CFST – A	152.4	3	50.8	M25
CFST – B	152.4	4.5	33.87	M25
CFST – C	152.4	6	25.4	M25

Table 8. Concrete filled GFRP tube CFFT column

Type of Specimen	Dia. of GFRP Tube (D_f)	Layers of GFRP Sheet	Thickness of GFRP tube, t_f (mm)	Aspect ratio (D_f/t_f)	Grade of In-filled Concrete

CFFT – A	152.4	4	3	50.8	M25
CFFT – B	152.4	6	4.5	33.87	M25
CFFT – C	152.4	8	6	25.4	M25

Table 9. Concrete filled Double tube section CFDTS column

Type of Specimen	Dia. of GFRP tube, D_f (mm)	Layers of GFRP Sheet	Thickness of GFRP tube (mm)	Aspect ratio, (D_f/t_f)	Dia. of steel tube, D_s	Thickness of steel tube (mm)	Aspect ratio, (D_s/t_s)	Grade of in-filled Concrete
CFDTS – A	152.4	4	3	50.8	86.4	1.5	57.6	M25
CFDTS – B	152.4	6	4.5	33.87	83.4	2.0	41.7	M25
CFDTS – C	152.4	8	6	25.4	80.4	2.5	32.16	M25

Results and discussion

Compression behavior of column specimens:

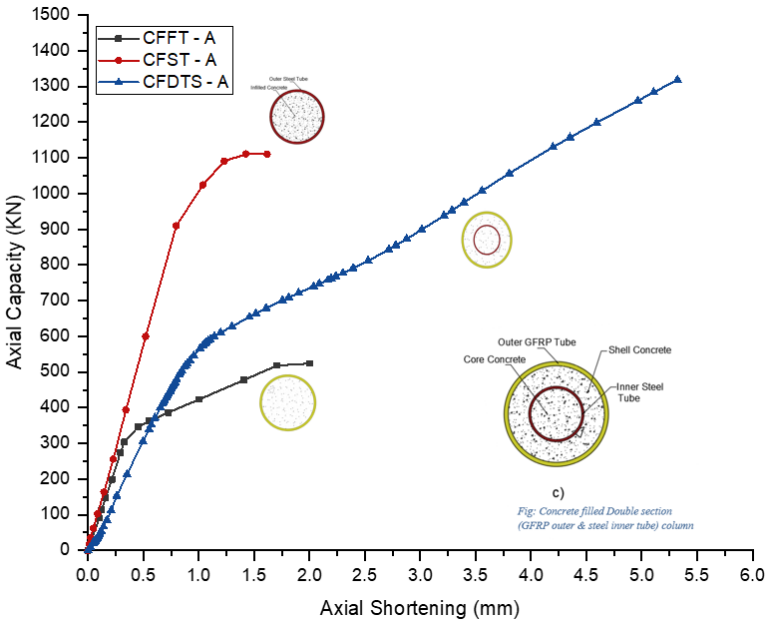

Fig (10): Load versus Axial Shortening for CFST-A, CFFT-A and CFDTS-A Column

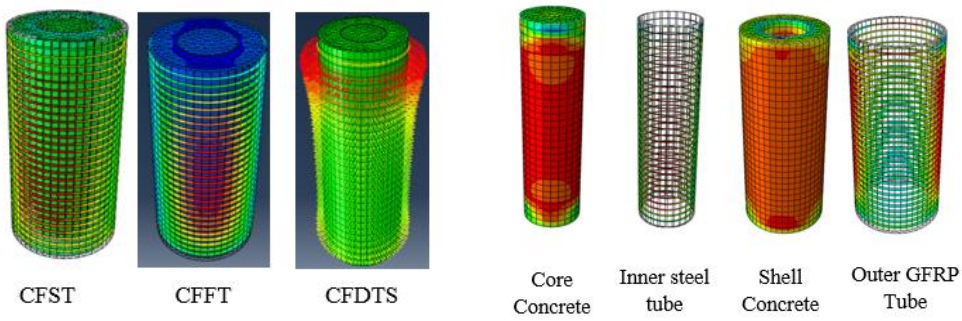

Fig (11): Stress Distribution

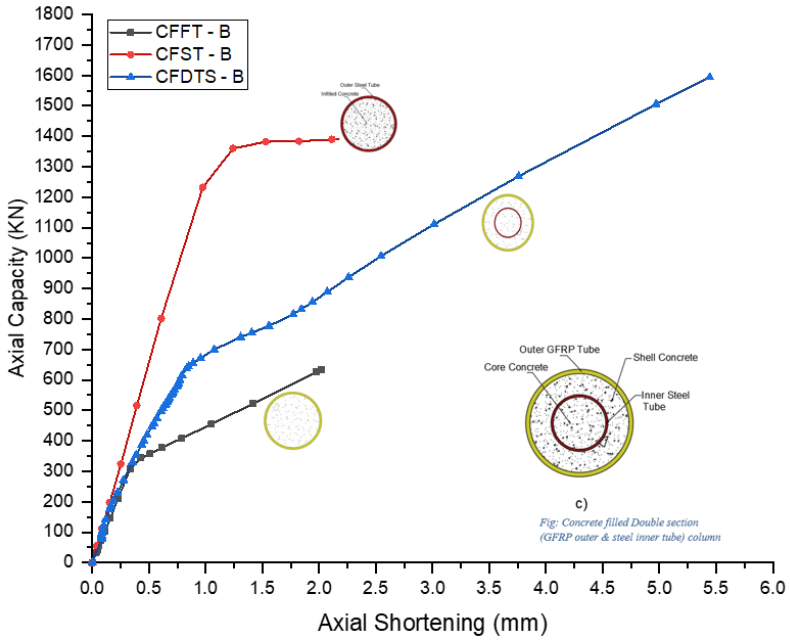

Fig (12): Load versus Axial Shortening for CFST-B, CFFT-B and CFDTS-B Column

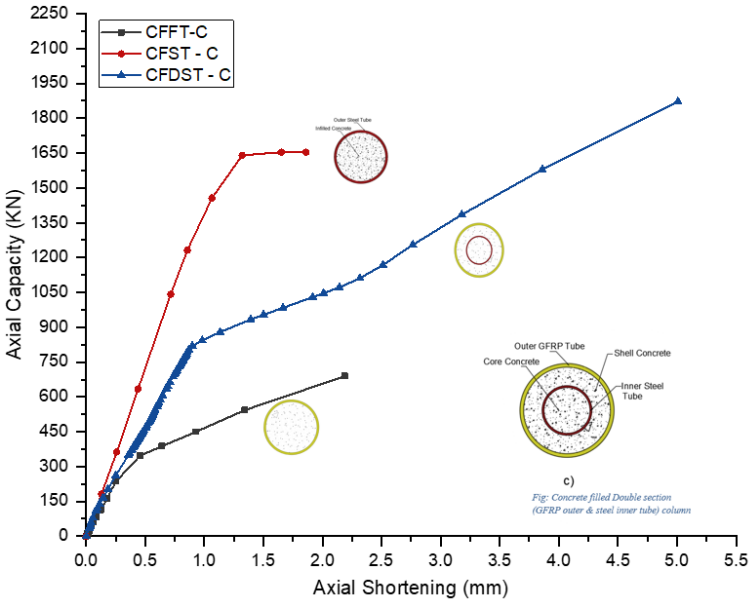

Fig (13): Load versus Axial Shortening for CFST-C, CFFT-C and CFDTS-C Column

Table 10: Properties of the column specimen and axial capacity from finite element analysis

Column Specimen	Grade of Shell & Core Concrete, fc (MPa)	Outer Tube Type	Outer Tube D (mm)	Outer Tube Thickness, t (mm)	Inner Tube Type	Inner Tube D (mm)	Inner Tube Thickness, t (mm)	Axial Compressive Capacity (KN)	Axial Stiffness (KN)
CFST - A	25	Mild Steel	152.4	3	----	----	----	1110.19	345313
CFST - B	25	Mild Steel	152.4	4.5	----	----	----	1404.30	400384
CFST - C	25	Mild Steel	152.4	6	----	----	----	1653.82	441037
CFFT - A	25	GFRP	152.4	3	----	----	----	523.70	281653
CFFT - B	25	GFRP	152.4	4.5	----	----	----	632.99	283955
CFFT - C	25	GFRP	152.4	6	----	----	----	689.66	285596
CFDTS - A	25	GFRP	152.4	3	Mild Steel	86.4	1.5	1318.52	180543
CFDTS - B	25	GFRP	152.4	4.5	Mild Steel	83.4	2	1593.73	208262
CFDTS - C	25	GFRP	152.4	6	Mild Steel	80.4	2.5	1872.12	266554

It could be observed from *table 10*, that double tube section columns CFDTS, exhibits greater compression capacity than its counterpart CFST column of same aspect ratios. The compression capacity of CFDTS – A (D_f/t_f=52.4) is 1318.52 KN which is +18% more than CFST– A (D_s/t_s=25.4). Similarly, CFDTS– B possess +13.5% more compression capacity than CFST– B. Similarly, CFDTS – C (D_f/t_f=33.87) exhibits +13.2% more compression capacity than CFST – C (D_s/t_s=33.87).

Above observations are strong evidence that Concrete Filled GFRP tube columns (CFFT, CFDTS) could be one of the best alternatives of CFST column based on axial compression capacity. The study also proved that the compression capacity could be achieved either by, altering aspect ratio (D/t) or by introducing steel tube of minimum thickness inside the concrete. Both of these are equally practicable and could be efficiently implemented.

1.3 Comparison of stress in steel tube: CFST – A, B & C and CFDTS – A, B & C

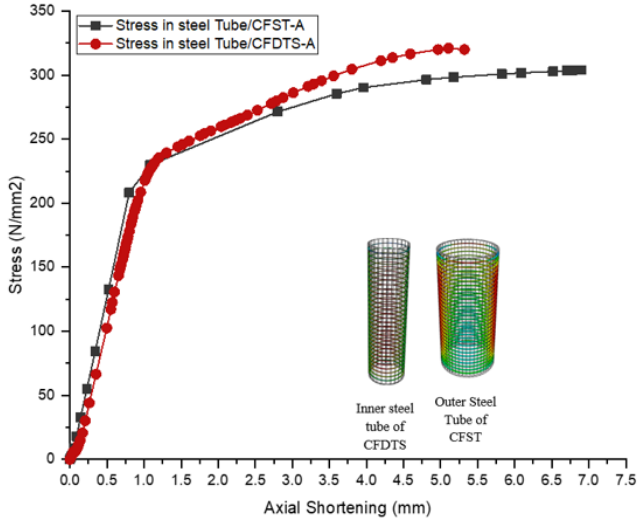

Fig (14): Stress versus Axial Shortening in steel tube CFST-A &CFDTS-A

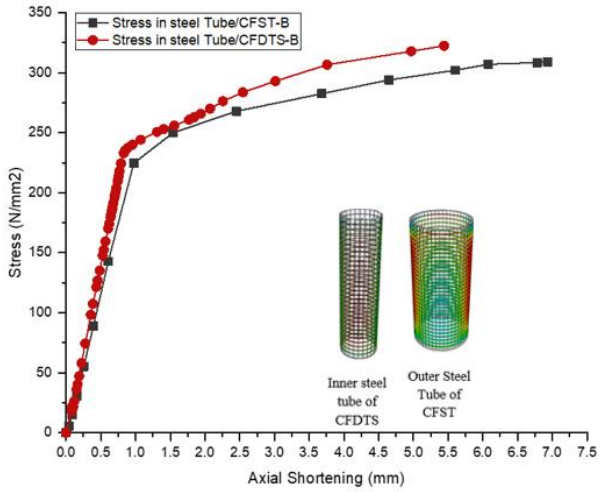

Fig (15): Stress versus Axial Shortening in steel tube CFST-B & CFDTS-B

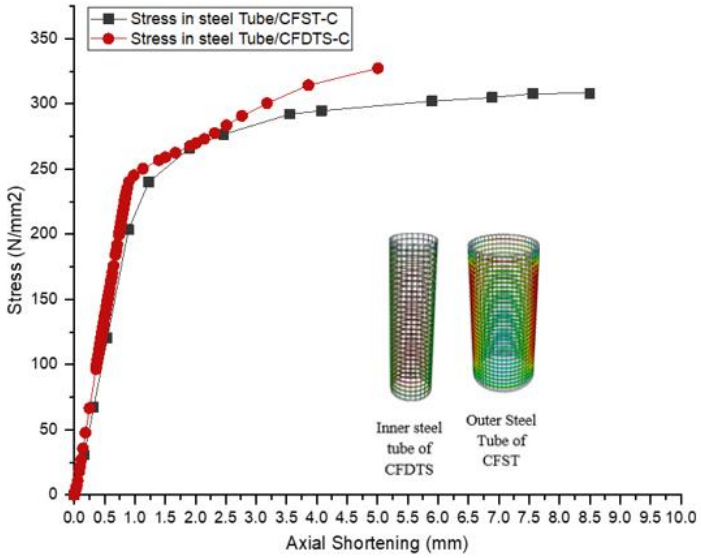

Fig (16): Stress versus Axial Shortening in steel tube CFST-C & CFDTS-C

Above figures illustrate comparison of stress in steel for the columns described in table 7, 8 and 9. The above comparison is for the aspect ratios, D_s/t_s =50.8, D_s/t_s =33.78 & D_s/t_s =25.4 & L/D = 2. It is observed that the stress in inner steel of CFDTS-A, B & C column is more than stress in outer steel of CFST-A, B & C column. The stress at failure in CFDTS-A is about 105% of stress in steel at failure of CFST-A column refer *fig (14).* The stress at failure in CFDTS-B is about 104% of stress in steel at failure of CFST-B column refer *fig (15).* The stress at failure in CFDTS-C is about 106% of stress in steel at failure of CFST-C column refer *fig (16).*

1.4 Performance based comparison of CFST, CFFT and CFDTS Column:

So far, the Finite Element Analysis based observations and illustrations revealed that CFFT column could be most suitable replacement of CFST column. The axial compression strength criteria of CFFT column could be increased by introducing inner steel tube inside the concrete in CFFT column in difficult design scenario. This composite structural member is known as CFDTS column. Therefore, there is a necessity of performance based comparison of classical CFST, CFFT and CFDTS column.

The axial load capacity of CFDTS's columns in *Table 10* signifies that axial load carrying capacity of CFDTS – A > CFSDT – B > CFDTS – C and reveals an important design parameter that the increase in confinement tube thickness and strength increases the Ultimate load at failure. Furthermore, from *fig (16)* the ductility parameter CFDTS column could be stated. The curve depicts that the CFDTS – C is more ductile in nature than CFDTS – B than CFDTS – A.

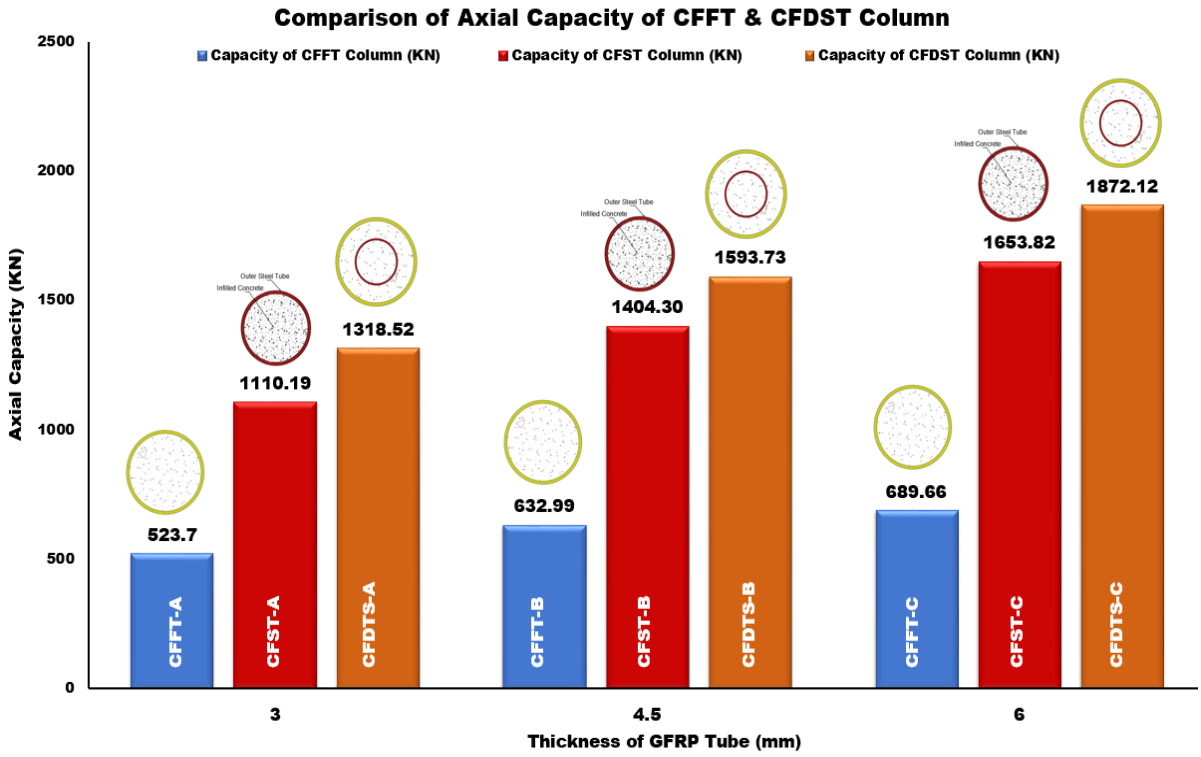

Fig (17) Comparison of Axial load carrying capacity of CFST, CFFT & CFDTS column

Conclusion

The project was aimed at numerical study of CFST, CFFT and CFDTS short columns. As the major objectives were to study the axial compression behavior of these short columns analytically and examine the best suitable alternatives of CFST column. The numerical study by using Finite Element Analysis software ABAQUS/CAE elucidate the important findings mentioned below.

Among columns of different specifications under consideration, CFDTS columns possess higher axial capacity than rest of the two categories of same aspect ratios i.e. CFDTS – A > CFST – A >CFFT – A. CFDTS – B > CFST – B > CFFT – B and CFDTS – C > CFST – C > CFFT – C. Therefore, the above study manifests that load carrying capacity of CFDTS's columns are superior to CFST's and CFFT's column.

References

ABAQUS. (2014). Abaqus 6.14. *Abaqus 6.14 Analysis User's Guide*, 14. http://130.149.89.49:2080/v6.14/books/usb/default.htm

Anitha Priyadharshani, S., Meher Prasad, A., & Sundaravadivelu, R. (2017). Analysis of GFRP stiffened composite plates with rectangular cutout. *Composite Structures*, *169*, 42–51. https://doi.org/10.1016/j.compstruct.2016.10.054

Hafezolghorani, M., Hejazi, F., Vaghei, R., Jaafar, M. S. Bin, & Karimzade, K. (2017). Simplified damage plasticity model for concrete. *Structural Engineering International*, *27*(1), 68–78. https://doi.org/10.2749/101686616X1081

Kopuri, N. A. G. K. M., & Priyadharshani, S. A. (2022). Materials Today : Proceedings Numerical analysis of concrete filled steel tube columns using ABAQUS. *Materials Today: Proceedings*, *xxxx*. https://doi.org/10.1016/j.matpr.2022.06.058

Li, G., Hou, C., Shen, L., & Yao, G. H. (2022). Performance and strength calculation of CFST columns with localized pitting corrosion damage. *Journal of Constructional Steel Research*, *188*(October 2021), 107011. https://doi.org/10.1016/j.jcsr.2021.107011

Mimiran, A., & Shahaway, M. (1997). Behavior of concrete column confined by fiber composites B Amir Mirmiran 1 and Mohsen Shahawy / Members , ASCE. *ASCE Journal of the Structural Engineering*, *123*(May), 583–590. https://doi.org/10.1061/(ASCE)0733-9445(1997)123:5(583)

Qasim S. Khan, M. Neaz Sheikh, M. N. S. H. (2020). Experimental results of circular FRP tube confined concrete (CFFT) and comparision with analytical models. *Journal of Building Engineering*, *29*. https://doi.org/10.1016/j.jobe.2019.101157